

Journal Pre-proof

Room temperature hydrogen sensing with Polyaniline/SnO₂/Pd Nanocomposites

Rohit Kumar Pippara, Pankaj Singh Chauhan, Anshul Yadav, Vinay Kishnani, Ankur Gupta



PII: S2590-0072(21)00007-1

DOI: <https://doi.org/10.1016/j.mne.2021.100086>

Reference: MNE 100086

To appear in: *Micro and Nano Engineering*

Received date: 21 January 2021

Revised date: 24 March 2021

Accepted date: 21 April 2021

Please cite this article as: R.K. Pippara, P.S. Chauhan, A. Yadav, et al., Room temperature hydrogen sensing with Polyaniline/SnO₂/Pd Nanocomposites, *Micro and Nano Engineering* (2021), <https://doi.org/10.1016/j.mne.2021.100086>

This is a PDF file of an article that has undergone enhancements after acceptance, such as the addition of a cover page and metadata, and formatting for readability, but it is not yet the definitive version of record. This version will undergo additional copyediting, typesetting and review before it is published in its final form, but we are providing this version to give early visibility of the article. Please note that, during the production process, errors may be discovered which could affect the content, and all legal disclaimers that apply to the journal pertain.

© 2021 The Author(s). Published by Elsevier B.V.

Room Temperature Hydrogen Sensing with Polyaniline/SnO₂/Pd Nanocomposites

Rohit Kumar Pippara¹, Pankaj Singh Chauhan², Anshul Yadav³, Vinay Kishnani⁴, Ankur Gupta^{4,*} ankurgupta@iitj.ac.in

¹School of Mechanical Sciences, Indian Institute of Technology Bhubaneswar, Odisha-752050, India

²Department of Mechanical Engineering, Indian Institute of Technology Kanpur, India

³Membrane Science and Separation Technology Division, CSIR-Central Salt and Marine Chemicals Research Institute, Bhavnagar - 364002, Gujarat, India

⁴Department of Mechanical Engineering, Indian Institute of Technology Jodhpur, Rajasthan-342037, India

*Corresponding Author:

Abstract

In this work, we report unique hybrid composite film fabricated with the amalgamation of metal, semiconductor and polymers for hydrogen sensing application at room temperature. Fabrication of a novel nanocomposite film based on tin oxide (SnO₂) nanosheets with polyaniline (PANI) doped with palladium (Pd) is performed using the hydrothermal synthesis technique. Functional aspects of the fabricated films are investigated with XRD, Raman spectra, FESEM, and FTIR spectral analysis. Interactions of the H₂ gas molecules with SnO₂, SnO₂-Pd, PANI, PANI-SnO₂, PANI-SnO₂-Pd nanocomposite are also theoretically studied. Using first-principles density functional theory, the effects of gas adsorption on the electronic and transport properties of the sensor are examined. The computations show that the sensitivity of the SnO₂ to the H₂ gas molecules is considerably improved after hybridisation with Pd and the sensitivity of the PANI to the H₂ gas molecules is considerably improved after hybridisation with SnO₂. Gas sensing characteristics of fabricated films of SnO₂, PANI and composite of SnO₂/PANI/Pd are also experimentally investigated at room temperature with varying concentration level ranging from 50 to 400 ppm. The highest sensitivity among all the films at room temperature has been observed as ~540% for the SnO₂/Pd film at 0.4% of the target gas and performance factor (the ratio of response percentage to total cycle time) is evaluated highest in Pd doped PANI-SnO₂ film. Our results reveal the promising future of SnO₂, PANI and Pd associated hybrid films in the development of ultra-high sensitive gas sensors.

Keywords

PANI; SnO₂; Gas Sensor; hydrogen sensor; DFT

1. Introduction

With the adverse condition of air quality and industrial necessitate, there is a burgeoning need for the implementation of high quality gas sensors, especially for environmental monitoring, control of harmful gases in domestic and industrial applications. Functionalised thin films play an important role to realise an efficient miniaturised gas sensing device. Previously, researchers have explored the various metals, combination of metal and semiconductor-based composite to add up the functionality as well as to enhance the high surface area to volume ratio in order to develop effective miniaturized gas sensors [1][2][3]. Still, efforts are required to overcome the limitation of semiconducting/metallic functional materials which often work at higher temperature range and offer several issues related to lesser sensitivity, high response time and reproducibility etc. Therefore, there is a colossal research scope for exploring and investigating the responses of various hybrid functional films as futuristic functional materials for gas sensing applications. The gas sensing properties are largely influenced by structural morphology and reactive groups present in the sensing film. Also, it is well known that the adsorption/desorption phenomenon in thin-film gas sensors has been the main cause of significant change in electrical properties. The sensing properties can further be enhanced by using doping materials which often act as a catalyst. Starting from the 1970s to till date, history of gas sensors has gone series of developments from semiconducting films to the extensive usage of polymeric films. Taguchi found that SnO₂ has several advantages and properties such as sensitivity, low operating temperature and a stable thermal structure [4]. In 1983, first conducting polymers named polypyrrole was ever reported for sensing ammonia [5]. Most of the harmful gasses are either oxidising or reducing in nature. Hence, different metal oxides are suitable for detecting these gases by electrical measurements. Various oxides have revealed gas response in the form of their resistance/conductance change viz., Chromium(III) oxide (Cr₂O₃), Manganese (III) oxide (Mn₂O₃), Cobalt(II, III) oxide (Co₃O₄), Nickel oxide (NiO), Copper(II) oxide (CuO), Strontium oxide (SrO), indium oxide (In₂O₃), Tungsten oxide (W₂O₃), Titanium dioxide (TiO₂), Vanadium Oxide (V₂O₃), Iron (III) oxide (Fe₂O₃), Germanium dioxide (GeO₂), Niobium oxide (Nb₂O₅), Molybdenum oxide (MoO₃), tantalum (Ta₂O₅), Lanthanum oxide (La₂O₃), Cerium Dioxide (CeO₂), and Neodymium(III) oxide (Nd₂O₃) etc. Furthermore, the metal oxide semiconductor-based gas sensing is based on the principle of change in resistance of surface electrical conductivity as a function concentration of the gas in the surrounding region. The adsorption/desorption of gas molecules on the surface of semiconductor takes place over the surface of the semiconductor metal oxide, which leads to redox reactions [6][7]. Tin oxide (SnO₂) and Zinc oxide (ZnO) films are the most widely studied materials under semiconductor-based gas-sensing applications. Gupta *et al.* reported ZnO nanostructures embedded in the polymeric matrix [8] and further doped with Pd for enhanced sensitivity for hydrogen sensing [9]. Out of functional materials used in commercially available MEMS-based gas sensors, some metal oxide semiconductors which are widely used are SnO₂ material, titanium oxide, tungsten oxide, copper oxide (CuO), iron oxide and indium oxide have also attracted much attention towards research.

Further, there are various types of polymers, including substituted polypyrroles ($H(C_4H_2NH)_nH$), polythiophenes (C_4H_2S)_n, polyindoles and polyanilines (PANI) but with less sensitivity and thermal stability. Functional modification of polymeric film is utmost essential in order to get better gas sensing properties. A detailed study is required to have a better gas sensor to optimise power consumption and performance. If a gas sensor works at room temperature, it will not only eliminate the cost of the heating arrangement, but also, it will directly reduce the power consumption as well as overall operating cost. To completely utilise the sensing properties of organic polymer films and inorganic metal oxides, composites of both are used. There are numerous kinds of hybrid Nanocomposite films with unique sensing properties. In order to enhance the sensitivity, researchers have explored various hybrid functional materials. It is well known that polymerised materials show a good response for adsorption/desorption of gas, and response can be further enhanced by chemical doping[10]. Till date, most of the research work in polymerisation was carried out on easily available organic monomer. Doped conducting polymers have much stability in the ambient environment. Doped polymers in the conductive state can be prepared directly with various techniques viz., plasma polymerisation or by the reaction of the monomer with Nitrosium hexafluorophosphate($NOPF_6$), or analogous salts, or directly by reacting with oxidising species for insertion of positive/negative ions in polymers etc. Choudhary HK. *et al.*[11] reported procedure to fabricate polyaniline with typical polymerisation process in which aniline and ammonium disulphate solution is used to transform to PANI. Furthermore, Li *et al.*[12] employed a hydrothermal route for the fabrication of and SnO_2 . Use of polymer film PANI/ SnO_2 was also explored for supercapacitor applications[13]. Nasresfahani S. *et al.*[14] investigated a facile hydrothermal route for the preparation of composite film of SnO_2 , reduced graphene oxide (rGO) and dopant as Pd for sensing of methane gas. Further, Kroutilet *et al.*[15] reported a methodology to prepare nanocomposite of PANI Films which was found useful for the evaluation of thin film for the gas sensor at a low cost.

In this work, SnO_2 , PANI and Pd are used for developing a novel composite film. Sensing films of SnO_2 , PANI and composite of $SnO_2 + PANI$ are also fabricated, and comparison for their gas sensing performance has been performed. Sensing characterisation has been performed at room temperature, varying ppm level of gas ranging from 50 to 400. The response of the film on the interaction of gas is investigated, and sensing properties are calculated from the response plots. The effect of doping materials and sensing mechanism is also discussed. Additionally, we used DFT study in order to analyse the electronic and transport properties of the SnO_2 , SnO_2 -Pd, PANI, PANI- SnO_2 PANI- SnO_2 -Pd hybrid nanosensor when in close proximity to the hydrogen gas molecules. Our results reveal the promising future of SnO_2 , SnO_2 -Pd, PANI, PANI- SnO_2 hybrid nanosensor in the development of ultra-high sensitive gas sensors.

2. Materials and Methods

2.1 Fabrication of SnO_2 Nanosheets

To synthesise SnO₂ sheets, various precursor such as stannous chloride (SnCl₂.2H₂O) purified, sodium hydroxide (NaOH) pellets, ethanol (C₂H₅OH) and DI water are used. Briefly, 5ml of ethanol solution was added to 15ml water in 80ml borosilicate beaker and was mixed properly followed by ultrasonication to get a lucid solution. Afterwards, 30mg of SnCl₂.2H₂O was added to the ethanol-based solution, and 0.3g NaOH was added gradually in 20ml water to get 0.4 M as a separate solution. The prepared solution was added in a dropwise manner to stannous chloride solution under continuous magnetic stirring until the pH of the solution reaches ~13. Then, the obtained mixture was transferred to a 100ml Teflon-lined stainless-steel autoclave and heated to 180° C for 12 hours inside a vacuum oven. After 12 hours, it is removed from the vacuum oven and kept in open environment till it reaches room temperature. The thick precipitate obtained through centrifugation was washed with deionised water and ethanol two times to completely remove chlorine ions. Finally, the light brown colour precipitate was dried in vacuum at 80°C for 1hr, and powdered light brown colour SnO₂ sheets were stored for further utilisation.

2.2 Fabrication of PANI

Materials required to fabricate PANI are aniline (C₆H₅NH₂), hydrochloric acid 1N (HCl), ammonium persulphate ((NH₄)₂S₂O₈), DI water. Chemical oxidation method was used for the synthesis of PANI. Typically, aniline is dissolved in acidic medium, and ammonium persulphate was used as an oxidising agent. Initially, 3ml aniline was added to 200ml HCl in a 500ml borosilicate beaker which was kept in an ice bath (at <5°C). This acidic solution is mixed properly to get a pale brown colour. Then, 11 grams of ammonium persulphate was dissolved in 100ml of DI water in a 250ml borosilicate container which was kept in an ice bath. It was mixed properly to get a transparent solution. Now, ammonium persulphate based solution was dropwise added to the acidic solution which was kept in an ice bath under constant stirring. Then, the blue colour solution was left in the ice bath for 8 hours. The final precipitate was obtained by centrifuging two times with DI water. To obtain a fine powder of PANI, the precipitate was kept in a vacuum oven at 70°C for 6 hours.

2.3 Fabrication of SnO₂/Pd

In order to synthesise SnO₂/Pd, 5ml of ethanol solution was added to 15ml water and mixed vigorously to get a clear solution. Then a ~30mg SnCl₂.2H₂O and 0.035g palladium dichloride (PdCl₂) was added to the above solution. The remaining procedure is the same as for pure SnO₂. At last, the precipitate was dried up in vacuum at 80°C for 1hr. The final Pd doped SnO₂ particles were observed to be in grey colour.

2.4 Fabrication of PANI/SnO₂

Materials required are aniline ($C_6H_5NH_2$), hydrochloric acid 1N (HCl), ammonium persulphate ($(NH_4)_2S_2O_8$), sodium dodecylbenzene sulphate ($C_{18}H_{29}NaO_3S$), SnO_2 in powdered form, DI water and ice bath ($0-5^\circ C$). To synthesise PANI/ SnO_2 , 4 grams of sodium dodecyl benzene sulphate ($C_{18}H_{29}NaO_3S$) was added to 70ml HCl in a 250ml glass beaker; the solution was mixed properly. Then 0.5 grams of SnO_2 powder and 1ml aniline ($C_6H_5NH_2$) was added to an acidic solution. The solution is mixed properly to get a yellow colour under magnetic stirring for half an hour so that SnO_2 particles are absorbed by the aniline. Now the solution was kept in an ice bath at $0-5^\circ C$. Then in a separate beaker 3.5 grams $(NH_4)_2S_2O_8$ was added to 30ml of DI water and kept in an ice bath. It was mixed properly to get a transparent solution. Now, the ammonium-based solution was added to the above solution drop by drop under constant stirring and the mixture was left in the ice bath for 6h. The dark greenish colour precipitate was obtained by centrifuging the mixture two times with deionised water. For obtaining fine powder of PANI/ SnO_2 , the precipitate was dried in a vacuum oven at $70^\circ C$ for 6hrs.

2.5 Fabrication of PANI/ SnO_2 +Pd

To fabricate PANI/ SnO_2 +Pd, 4 grams of ($C_{18}H_{29}NaO_3S$) was added to 70ml HCl solution. Then 0.5 grams of SnO_2 /Pd powder and 1ml aniline was added to an acidic solution. The solution is mixed properly to get a grey colour mixture. The remaining procedure is the same as for the PANI/ SnO_2 composite.

2.6 Computational details

The adsorption of H_2 gas molecules on SnO_2 , SnO_2 -Pd, PANI, PANI- SnO_2 and PANI- SnO_2 -Pd hybrid nanostructure was studied by the density functional theory (DFT) calculations. The full geometry optimisations and energetic calculations, and Mulliken population analyses were carried out. The Perdew, Burke, and Ernzerhof (PBE) approach of generalised gradient approximation (GGA) is used for the exchange-correlation function. The adsorption energy provides us a quantitative explanation of the interaction strength between adsorbent and adsorbate. The complexes formed are completely relaxed. The adsorption energies of the hydrogen gas molecules on the SnO_2 , SnO_2 -Pd, PANI, PANI- SnO_2 system are obtained by:

$$E = E_{gas-adsorbate} - E_{adsorbate} - E_{gas}$$

where $E_{gas-adsorbate}$ is the total energy of the gas molecule–adsorbate compound, $E_{adsorbate}$ is the energy of an isolated adsorbate system and E_{gas} is the energy of an isolated gas molecule.

2.7 Gas Sensing Set-up

To investigate the sensing characteristics, gas sensing set up was utilised, schematic of which is shown in figure 1. Fabricated sensing films were coated over interdigitated electrodes on the Si substrate. Electrodes were connected for resistance measurements to an electrometer (6517A, Keithley Instruments). Set-up is equipped with power supply, temperature control unit, mass flow

controllers, interfaced with a computer. A fixed voltage of 1 V was applied for the resistance measurements. Sensing chamber is attached to a vacuum pump for air contamination removal purpose.

Figure 1. Schematic representation of gas sensing set-up. 1. Outlet gas pressure indicator, 2. Air sealed chamber boundary, 3. Gas outlet indicator, 4. Temperature controlled stage, 5. Sensing film kept over the stage, 6. Mass flow controller 1 (MFC 1), 7. Mass flow controller 2 (MFC 2), 8. Gas cylinder 1, 9. Gas cylinder 2

3. Results and Discussion

3.1 DFT calculations:

We first optimize the SnO₂, SnO₂-Pd, PANI, PANI-SnO₂ and PANI-SnO₂-Pd hybrid nanostructure using DFT calculations in order to obtain the most energetically stable geometry of the sensor.

Figure 2. DFT Optimized geometries of (a) SnO₂ (b) SnO₂-Pd (c) PANI (d) PANI-SnO₂-Pd, hybrid nanosensor (black = carbon, grey = hydrogen, red = oxygen, purple = zinc, white = silver, blue = nitrogen, dark blue = palladium)

Next, the adsorption mechanisms of the H₂ gas molecule onto a SnO₂, SnO₂-Pd, PANI, PANI-SnO₂ and PANI-SnO₂-Pd nanostructures are addressed. The adsorption energies of the gas molecules on the nanostructures and the minimum binding distances are summarised in Table 1.

Table 1. The calculated adsorption energy (E_{ad}), binding distance (d) which is the shortest atom to atom distance between the molecule and the sensor

System	E_{ad} (eV)	d (Å)
H ₂ and SnO ₂	- 0.09 eV	2.16
H ₂ and SnO ₂ -Pd	- 0.46 eV	1.82
H ₂ and PANI	- 0.003 eV	3.18
H ₂ and PANI-SnO ₂ -Pd	- 0.13 eV	2.2

The DFT studies show that for H₂ gas sensing, the order of adsorbing capacity is SnO₂ < SnO₂-Pd < PANI < PANI-SnO₂ < PANI-SnO₂-Pd.

Figure 3. Interaction of H₂ with (a) SnO₂ (b) SnO₂-Pd (c) PANI (d) PANI-SnO₂-Pd

(black = carbon, grey = hydrogen, red = oxygen, purple = zinc, white = silver, blue = nitrogen, dark blue = palladium)

3.2 Structural Characterization

3.2.1 FESEM and EDAX analysis

SEM images for the prepared films are shown in Figure 4. From figure 4(a) SEM image shows honeycomb type granular surface morphology of PANI with the presence of some nanofibres. From Fig. 4(b), it is observed that the pure SnO₂ nanosheets are well grown and have an approximate length of 200 nm. The morphologies of PANI/SnO₂ nanocomposite were also examined by SEM, as shown in Fig. 4(c) & 4(d). The irregular nanostructured PANI layer is coated over the surface of SnO₂. While, Fig. 4(e) and (f) shows the PANI and Pd doped SnO₂ nanosheet. These images confirm the successful fabrication of nanosize heterostructure of Pd doped SnO₂/PANI nanocomposite.

Figure 4: SEM images for the prepared films: (a) Poly aniline (PANI), (b) Tin oxide (SnO₂), (c) & (d) PANI doped-Tin Oxide (PANI-SnO₂) and (e) & (f) PANI and Pd doped SnO₂.

3.2.2 RAMAN Spectroscopy

Raman spectroscopy provides information regarding the quality and defect states of all the prepared thin films. Vibrational, rotational, and other low frequency modes in a unit cell of compound (SnO₂) can be observed in the Raman spectra. Fig. 5(a) shows the Raman spectra of the prepared SnO₂ nanosheet material. The strong peaks at 500 cm⁻¹ are associated with the expansion, 630 cm⁻¹ due to contraction of vibration mode of Sn-O bonds. In addition, an intense peak at around 234 cm⁻¹ in the SnO₂ nano sheets confirms the change in the phase, which is not found in the bulk phase of SnO₂ crystals [16]. Figure 5(b) illustrates the spectra of the SnO₂ + Pd samples. The similar features of the spectra were detected in the region 400–1200 cm⁻¹ wave number. The most intense peaks at 480 cm⁻¹, 571 cm⁻¹ are due to Sn-O bonds. A peak at 1073 cm⁻¹ is due to the presence of Pd in the film [17]. Compared with SnO₂ nanosheets, the Raman spectra of SnO₂+Pd samples exhibit measurable line shifts and broadening. This behaviour is due to the decrease of SnO₂ crystal size. It is well known that Heisenberg uncertainty principle provides a relation between photon position Δx and photon momentum Δp . The mathematical expression is given as:

$$\Delta p \Delta x \geq \frac{h^2}{4}$$

where the particle size is given by Δx and the particle momentum distribution is given by Δp . 'h' is constantly given by Planck. As the crystalline size of a substance reduces, the more molecules get composed inside a particle, and thus the molecules momentum distribution rises respectively. This

broadening is due to the law of conservation of momentum. This molecular dispersion causes nonsymmetric broadening and might shift band to lower wave number[18].

Figure 5: Raman spectra of a) SnO₂ Nanosheet and b) SnO₂ + Pd samples.

Fig. 6(a) illustrates the Raman spectra of PANI. The chemical structure of the polyaniline is benzenoid or quinonoid or both. If an equal amount of both types of structures is present, then it is called emeraldine. The dopants added in polymer significantly influence the intensity of RAMAN peaks. An intense peak due to the stretching vibration of C≡N-type quonoid di-imine structure appeared at 1500 cm⁻¹. The sharp peak at 1187 cm⁻¹ is due to the presence of C–N bond and a peak at 1607 cm⁻¹ due to C–C bond[19]. Figure 6(b) illustrates the Raman spectrum of SnO₂+PANI. The intense peak of C–C bond appears at 1639 cm⁻¹, C–N bond at 1188 cm⁻¹, and C≡N bond appears at 1429 cm⁻¹. A sharp peak corresponding to Sn–O bond is evident at 818 cm⁻¹. This result shows that the film of SnO₂+PANI has a combination of properties of polyaniline and tin oxide.

Figure 6: Raman spectra of a) PANI and b) SnO₂ + PANI samples.

Fig. 7 illustrates the Raman spectral analysis of hybrid nanocomposite film of Pd, SnO₂, and conductive PANI. From Fig. 7(a) the hybrid composite film SnO₂+Pd/PANI shows a peak at 486 cm⁻¹ corresponding to Sn–O bonds. The three sharp peaks at 1187 cm⁻¹, 1324 cm⁻¹, 1629 cm⁻¹ due to C–N bonds, C≡N bonds and C–C bonds respectively. Fig. 7(b) illustrates the Raman spectroscopy of all the prepared thin films for comparison. From Fig. 7(b), it can be observed that the intensity of peak reduces as the size of the crystal increases with doping which provides less scattering in Raman spectroscopy. The shift in wavelength and broadening is noticed, which can be understood on the basis of the Heisenberg uncertainty principle.

Figure 7: Raman spectra of a) SnO₂+Pd/PANI and b) combined spectra of all the films.

3.2.3 XRD Analysis

The X-ray diffraction of the prepared SnO₂ is shown in Fig. 8 (a). It is clear for XRD graph that the prominent peaks are present at 2θ= 27°, 32° and 52° and corresponds to (110), (101), and (211) planes of the standard rutile structure of SnO₂(JCPDS 41–1445)[20]. The (101) peak is comparatively stronger than (110), which suggests that (101) is the growth direction of the nanomaterial. It provides support in the argument of better gas sensing performance as the surface of (101) has high specific energy. Fig. 8(b) shows the XRD analysis of SnO₂+Pd. The noticeable intense peaks can be identified at 27°, 32° and 52° which are attributed to (110), (101) and (211) planes of SnO₂. Another sharp peak observed at 46° corresponds to the presence of Pd in the sample[20].

Figure 8: a) X-Ray diffraction of SnO₂ Nanosheet and b) XRD of doped SnO₂ + Pd.

Fig. 9a shows the XRD diffraction patterns of the synthesised PANI film. In pure PANI, one broadpeak can be observed at 23°, which is attributed to the distinguishing peak of powdered form of PANI. This confirms the lower crystalline and conductive structure of polyaniline. Fig. 9(b) shows an XRD analysis of SnO₂ + PANI film. The peak corresponding to PANI overlapped with the peak of SnO₂ and showed a combined broad peak at 27° indicated by (110) plane. The other peaks do not show any response due to addition of PANI in SnO₂.

Figure 9: a) X-Ray diffraction of PANI and b) SnO₂ + PANI nanocomposite.

Fig. 10 shows the XRD patterns of SnO₂+Pd/PANI nanocomposite. In this hybrid composite film, an intense peak at 32° is obtained which is attributed to (101) plane of SnO₂. Some other peaks at 27°, 34°, 52°, 62° and 65° which are attributed to (110), (200), (210), (310), and (301) planes of SnO₂, Pd, and PANI. The XRD analysis confirms the nanocomposite formation.

Figure 10: a) X-Ray diffraction of SnO₂ +Pd/ PANI.

3.2.4 FTIR Analysis

In order to understand the chemical bonding of the prepared nanocomposite, FTIR was conducted in the wavelength range of 0–4000 cm⁻¹ and shown in Fig. 11. Fig. 11(a) shows the FTIR of Pd doped SnO₂ thin film. The stretching vibration of the surface hydroxyl group has a sharp peak at 3384 cm⁻¹. The peak observed at 1604 cm⁻¹ is related to the Sn–OH bond. The peaks appeared between 500 cm⁻¹ and 600 cm⁻¹ is related to the O–Sn–O bridge of SnO₂. No other extra peaks were detected in the Pd doped SnO₂ sample. From Fig. 11 (b), the bands appearing at 479 cm⁻¹ and 583 cm⁻¹ are due to the vibration of symmetric Sn–O–Sn and vibration of anti-symmetric Sn–O–Sn or O–Sn–O groups of SnO₂. The peak at 1604 cm⁻¹ is due to Sn-OH bond. These peaks confirm the presence of SnO₂.

Figure 11: a) FTIR of SnO₂/Pd and b) FTIR of SnO₂.

The FTIR spectra of pure PANI, PANI+SnO₂, and PANI+ SnO₂/Pd are shown in Fig. 12. From fig. 12(a), the sharp absorption peak at 792 cm⁻¹ is due to the out-of-plane bending vibration of the N–H bond. Presence of benzenoid band around 1486 cm⁻¹ and C=N (quinonoid) vibration around 1576 cm⁻¹ indicate the emeraldine salt form of polyaniline. The band at 3374 cm⁻¹ indicates the widening of N–H bond of the aromatic ring of PANI. The stretching of C–N band at aromatic amine appears at 1274 cm⁻¹. The absorption band of N=Q=N vibration (where Q denotes the quinoid ring) is at 1156 cm⁻¹. While, the C–H stretching vibration in the open-chain is evident by the peaks at 2924 cm⁻¹ and 3343 cm⁻¹.

Fig. 12(b) shows the FTIR spectrum of PANI/SnO₂. The stretching between Sn–O–Sn is symmetric. This symmetric band appears at 575 cm⁻¹. The protonated form of PANI has a characteristic peak at

1287 cm^{-1} which shows conducting properties. The intense band of C–H bond has in-plane bending vibration at 1156 cm^{-1} . Furthermore, the transmittance peaks at 1565 and 1445 cm^{-1} are attributed to the distinguishing peaks for PANI. The stretching mode of C=N bond appearing at 1565 cm^{-1} and the stretching mode vibration band of C=C bond at 1445 cm^{-1} , corresponds to PANI. The stretching of the C–N bond in the benzenoid ring has a peak at 1314 cm^{-1} . At the same time, the peak at 812 cm^{-1} indicates the C–H-bond. From fig. 12(c), FTIR of polyaniline PANI/SnO₂ + Pd shows similar peaks but with low transmittance. There are no extra peaks in the Pd-doped samples; this suggests Pd dopant used occupied a substituent place in the lattice of SnO₂. As compared to pure PANI, PANI/SnO₂ and PANI/SnO₂ + Pd composite shows a reduction in the ratio of intensity due to benzenoid and quinonoid structure. This indicates prepared nanocomposite film is in a more stabilised form, and it can be related to high sensing performance of the material.

Figure 12: a) FTIR of PANI, b) PANI+SnO₂ and c) FTIR of PANI+SnO₂ + Pd.

3.3 Gas Sensing Characterisation:

It is observed that all the thin film gas sensors show dynamic response with 50 ppm of H₂ gas at room temperature, as shown in Fig. 13. The electrical resistance of the gas sensing film increases in the presence of H₂ gas and again reduces to a lower saturated value when the gas is removed from the test chamber, which completes one cycle. We have recorded several such cycles which are shown in Fig. 13. There is a shift in baseline resistance (the lower saturated resistance value) is observed with an increase in a number of sensing cycles. This is attributed to the retention of some of the H₂ gas molecules by the sensing film.

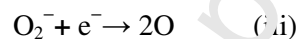
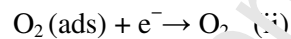
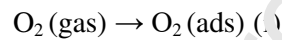
Figure 13: Resistance vs Time graph for a) PANI, b) SnO₂, c) SnO₂ + Pd and d) SnO₂ +Pd/PANI with H₂ at 50ppm

Figure 14: Resistance vs. Time graph for a) PANI, b) SnO₂, c) SnO₂ + Pd and d) SnO₂ +Pd/PANI with H₂ at different ppm.

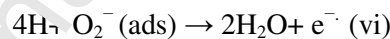
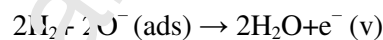
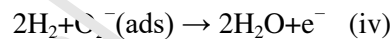
As the mass flow controller of gas is switched on, the resistance of the sensor increases till it reaches a saturation level, and when the gas is switched off, the resistance is dropped to initial resistance. From the fig. 13 and 14, it is observed that all the thin films show cyclic response with the interaction of H₂ gas. The SnO₂ and SnO₂+Pd sensing films show repeatability as it reaches to the initial value when the gas supply is switched off. But in the case of PANI and SnO₂ +Pd/PANI films are showing least repeatability. The use of Pd in gas sensing has increased the sensitivity of the gas sensor. It is based on the fact that Pd exists in FCC crystal lattice and has octahedral space in its interstitial space. These spaces are appropriate enough for H₂ molecules to get adsorbed. Pd also acts as a catalyst for the dissociation of H₂ gas molecules into

H atom and forms PdH_x. That is why hydrogen gas shows great affinity towards Pd and shows a higher response in comparison to pure SnO₂.

From the fig. 14, it has been observed that all the thin films show cyclic response with the interaction of H₂ gas even at different levels of ppm. The sensing films SnO₂ and SnO₂ + Pd showed repeatability even when the ppm level of H₂ gas changed. But the film made up of PANI show least repeatability. We can also observe the increase in saturation resistance with the increase in ppm level of gas. From figure 13 and 14, it is observed that the resistance of SnO₂ and SnO₂ + Pd film increases evidently with high stability when H₂ gas is passed. The sensing mechanism of SnO₂ and SnO₂ + Pd is due to reduction of H₂ with the oxygen O₂ molecules on the surface of the sensor film. The SnO₂ and SnO₂+Pd absorb oxygen species from the atmosphere to the film surface [21][22][16]. These absorbed O₂ molecules capture the free electrons from the surface of metal oxide composite and form negative oxygen species which increases the surface resistance as shown in the following reactions:



H₂ gas molecules are dissociated to H atom on interaction with different adsorbed negative oxygen species. This results in an increase of electron concentration, and the resistance of tin oxide SnO₂ film increases. The chemical reactions of H atom with negative oxygen species near the solid-gas interface are given below:



The resistance of SnO₂ is reduced to initial resistance when the film is exposed to ambient air. Ambient air has oxygen species which react with the adsorbed hydrogen atom on the surface of the film to decrease the resistance of the film. By using Pd with SnO₂ assists in the dissociation of H₂ molecule quickly, which results in an increase in sensitivity of SnO₂+Pd film. It can be concluded that by using Pd with SnO₂, there is an enhancement for sensing of H₂ gas which can be clearly observed in sensing results.

Figure 15 shows the reaction schematic to understand the interaction of hydrogen with polyaniline. The gas sensing mechanism of PANI and SnO₂+Pd/PANI is due to reduction of H₂ molecule with the amine (-NH-) and imine (=N-) groups. PANI has an equal number of amine (-NH-) and imine (=N-) groups. The imine (=N-) group bonds with the H atom, which increases the resistance of the polymer film due to protonation of N atom. The equation is shown below:

Figure 15 shows the reaction mechanism during the interaction of hydrogen with aniline.

When ambient air is passed over the film, this NH⁺ group loses the H atom and comes back to initial imine (=N-) groups. We also observe that PANI and SnO₂+Pd/PANI show the least stability as PANI

is a P-type semiconductor. In a P-type semiconductor, the number of holes is more than the number of electrons. So, when the ambient air is passed, all the NH^+ group does not form initial imine ($=\text{N}-$) groups. Because SnO_2+Pd film has more sensitivity than PANI, which can be observed from sensing results. The composite film $\text{SnO}_2+\text{Pd}/\text{PANI}$ has both oxygen and imine ($=\text{N}-$) groups which gives a quick response when interacted with gas at low ppm.

In SnO_2/PANI nanocomposite material SnO_2 is an n-type and PANI is a p-type material. During the hydrothermal synthesis method, oxygen vacancies/defects are created on the surface of SnO_2 . Under the normal atmospheric condition, the environmental oxygen gets adsorbed on the surface of SnO_2 by occupying the space of oxygen vacancies. These adsorbed oxygen molecules capture the free electrons present on the conduction band of SnO_2 semiconductor and create a depletion region. Capturing of electrons increases the material resistance and decreases the number of majority charge carriers, i.e. electrons. While PANI behaves as a p-type semiconducting material with holes as the majority charge carrier. Hence, the composite of SnO_2 and PANI, due to the capturing of free electrons of SnO_2 and holes as a majority charge carrier in PANI, have an overall tendency to behave as a p-type semiconductor. The p-type behaviour of the SnO_2/PANI nanocomposite is evident from our sensing results, wherein the presence of H_2 gas molecules, the resistance of the material starts increasing. Following a well-known detection mechanism, H_2 gas molecules react with adsorbed oxygen species (O^-/O^{2-}) and form a water molecule with releasing of free electrons. These free electrons now recombine with the holes which are the majority charge carriers of the nanocomposite. This charge neutralisation reduces the number of charge carriers, i.e. holes and increases the resistance of the material. In this process, the Pd nanoparticles act as a catalyst for the adsorption of hydrogen gas molecules onto the surface of metal oxide. Pd nanoparticles dissociate H_2 molecule into H atom and form PdH_x . Pd nanoparticles actively participate in electron exchange with metal oxide semiconducting material (SnO_2 in our case). H atom in Pd lattice act as electron scattering element [22]. Hence, in the presence of H_2 gas, the Pd coating increases the resistance of the sensing material. Figure 16 shows the comparison of various functional films for their response percentage.

Figure 16 shows the comparison of the response percentage of different materials for different concentration of H_2 gas.

4. Discussions

4.1 Sensitivity

The change in resistance of sensing film with respect to the initial resistance when the interaction of gas with the interaction of gas is known as sensitivity. Sensitivity is calculated by an equation:

$$\text{Sensitivity (S)} = \frac{R-R_0}{R_0} * 100,$$

where R is the instantaneous resistance when gas interacts with the film, R_0 is resistance at initial state when there is no interaction of gas. The values for instantaneous resistance and initial resistance are calculated, and values in tabulated form can be referred from supplementary information. Figure 17 represents the variation of the sensitivity values with respect to cycle.

Figure 17: Sensitivity vs cycle graph a) at 50 ppm, b) different ppm for H_2 gas (cycle-1 indicates 50 ppm (1-50 ppm), 2 indicates 100 ppm. Similarly, 3-150 ppm, 4-200 ppm, 5-250 ppm, 6-300 ppm, 7-350 ppm, 8-400 ppm.

From Fig. 17, it is observed that the composite with SnO_2+Pd shows the highest sensitivity in comparison to the SnO_2 film and $SnO_2+Pd+PANI$ film. At a low level of ppm, the film made of SnO_2 shows high sensitivity and the PANI film shows the least sensitivity when interacted with H_2 gas.

4.2 Response and Recovery time

Response Time is defined as the time required for a sensor to reach ~90% of the total response of the resistance upon exposure to the target gas. Recovery time is defined as the time required for a sensor to return to 90% of the original initial resistance on the removal of the target gas. The response time, i.e. X_1 depicted in the figure 18 as well as recovery time i.e. X_2 as indicated in the figure 18 have been evaluated to estimate the performance factor of the reported films.

Figure 18. X_1 - Response time and X_2 - The recovery time for SnO_2+Pd with H_2 gas.

From fig. 19, as shown below, the film made up of PANI shows a quick response and recovery time when interacted with gas. The composite $SnO_2+Pd/PANI$ also shows a good response and recovery with H_2 gas at a different level of ppm. At low ppm, the composite has a response of 30 seconds and a recovery time of 50 seconds. But the film made up of the only SnO_2 has more response time and recovery time.

Figure 19: a) Recovery vs cycle graph at different ppm, b) Response vs cycle graph at different ppm (50 to 400) with H_2 gas.

4.3 Performance Factor

Performance Factor has been evaluated by the ratio of sensitivity to total cycle time. Total time can be calculated as the summation of response time and recovery time. From figure: 20 below, we can observe that the performance of Polymer composite is higher than other films at low ppm and at high ppm.

Figure 20: Performance factors of all films with H_2 gas.

Table 2. H_2 gas sensing comparison for different PANI/ SnO_2 based composites

Sensor Type	H ₂ Concentration (%)	Sensitivity (%)	Response/recovery time(s)	Temperature (K)	Reference
MWCNT/PANI	0.4	24	48/55	273	[24]
Graphene/PANI	1	16.57	-	Room Temperature	[25]
PANI		9.38		Room Temperature	
Graphene		0.83			
PANI nanofibre	1	-	8/60	Room temperature	[26]
PANI/SnO ₂	6000 ppm	42	11/7	303	[27]
Al-SnO ₂ /PANI	1000 ppm	-	2/2	321	[28]
TiO ₂ /PANI	-	43	140/-	Room temperature	[29]
Nanocrystalline SnO ₂ thin film	1000 ppm	600	205/116	Room temperature	[30]
Pd decorated SnO ₂	10,000 ppm	1.2×10^5	~2 Sec (response time)	Room temperature	[31]
SnO ₂	400 ppm	391	142/156	Room temperature	
SnO ₂ /Pd	400 ppm	546.14	547/164	Room temperature	This work
Pd-SnO ₂ /PANI	50ppm	19.2	39/53	Room Temperature	
	350 ppm	353.7	141/76	Room Temperature	

Conclusions

This work reports the novel functionalised film with a unique combination of metal-semiconductor-polymer for gas sensing application. The sensing response of the SnO₂/Pd film on gas interaction at room temperature has been observed with highest sensitivity while, the performance factor is evaluated highest in Pd doped PANI-SnO₂ film. In this study, we also reported DFT calculations to characterise the interaction between H₂ gas molecule onto SnO₂, SnO₂-Pd, PANI, PANI-SnO₂ and PANI-SnO₂-Pd nanostructures.

Acknowledgements

Authors would like to express sincere thank to Prof. Shantanu Bhattacharya, Mechanical Engineering Department, Indian Institute of Technology, Kanpur, India for providing assistance in gas sensing characterisation.

Declaration of interests

The authors declare that they have no known competing financial interests or personal relationships that could have appeared to influence the work reported in this paper.

The authors declare the following financial interests/personal relationships which may be considered as potential competing interests:

References

- [1] A. Gupta, A. Srivastava, C. J. Mathai, K. Gangopadhyay, S. Gangopadhyay, and S. Bhattacharya, “Nano porous palladium sensor for sensitive and rapid detection of hydrogen,” *Sens. Lett.*, vol. 12, no. 8, pp. 1279–1285, Aug. 2014, doi: 10.1166/sl.2014.3307.
- [2] K. Mondal, B. Balasubramaniam, A. Gupta, A. A. Lahcen, and M. Kwiatkowski, “Carbon Nanostructures for Energy and Sensing Applications,” *Journal of Nanotechnology*, vol. 2019. Hindawi Limited, 2019, doi: 10.1155/2019/1454327.
- [3] A. Gupta, S. S. Pandey, and S. Bhattacharya, “High aspect ZnO nanostructures based hydrogen sensing,” in *AIP Conference Proceedings*, Jun. 2013, vol. 1576, no. 1, pp. 291–292, doi: 10.1063/1.4810215.
- [4] N. Taguchi, A. E. Myer, and A. E. Geoffrey, “Gas Detective Device,” *US Pat.*, no. 54, pp. 1–5, 1971.
- [5] “Nylander: An ammonia detector based on a conducting polymer - Google Scholar.” https://scholar.google.com/scholar?cluster=1020262609294158664&hl=en&as_sdt=2005&sciodt=0,5#d=gs_cit&u=%2Fscholar%3Fq%3Dinfo%3A%2Fgtz0_ZnU94J%3Ascholar.google.com%2F%26output%3Dcite%26scirp%3D0%26scfhb%3D1%26hl%3Den (accessed Jan. 17, 2021).
- [6] A. Gupta, P. K. Parida, and P. Pal, *Functional Films for Gas Sensing Applications: A Review*, Springer, Singapore, 2019, pp. 1–37.
- [7] P. Pal, A. Yadav, P. S. Chaudhary, P. K. Parida, and A. Gupta, “Reduced graphene oxide based hybrid functionalized films for hydrogen detection: Theoretical and experimental studies,” *Sensors Int.*, vol. 2, p. 100072, Jan. 2021, doi: 10.1016/j.sintl.2020.100072.
- [8] A. Gupta, S. S. Pandey, M. Nayak, A. Maity, S. B. Majumder, and S. Bhattacharya, “Hydrogen sensing based on nanoporous silica-embedded ultra dense ZnO nanobundles,” *RSC Adv.*, vol. 4, no. 15, pp. 7476–7482, Jan. 2014, doi: 10.1039/c3ra45316b.
- [9] A. Gupta, S. Gangopadhyay, K. Gangopadhyay, and S. Bhattacharya, “Palladium-Functionalized Nanostructured Platforms for Enhanced Hydrogen Sensing,” *Nanomater. Nanotechnol.*, vol. 6, p. 40, Jan. 2016, doi: 10.5772/63987.
- [10] J. J. Miasik, A. Hooper, and B. C. Tofield, “Conducting polymer gas sensors,” *Journal of the Chemical Society, Faraday Transactions 1: Physical Chemistry in Condensed Phases*, vol. 82, no. 4. The Royal Society of Chemistry, pp. 1117–1126, Jan. 01, 1986, doi: 10.1039/F19868201117.
- [11] H. K. Choudhary, R. Kumar, S. P. Pawar, A. V. Anupama, S. Bose, and B. Sahoo, “Effect of Coral-Shaped Yttrium Iron Garnet Particles on the EMI Shielding Behaviour of Yttrium Iron Garnet-Polyaniline-Wax Composites,” *ChemistrySelect*, vol. 3, no. 7, pp. 2120–2130, Feb. 2018, doi: 10.1002/slct.201702698.

- [12] Y. Li, Y. Guo, R. Tan, P. Cui, Y. Li, and W. Song, "Synthesis of SnO₂ nano-sheets by a template-free hydrothermal method," *Mater. Lett.*, vol. 63, no. 24–25, pp. 2085–2088, Oct. 2009, doi: 10.1016/j.matlet.2009.06.060.
- [13] Z. A. Hu, Y. L. Xie, Y. X. Wang, L. P. Mo, Y. Y. Yang, and Z. Y. Zhang, "Polyaniline/SnO₂ nanocomposite for supercapacitor applications," *Mater. Chem. Phys.*, vol. 114, no. 2–3, pp. 990–995, Apr. 2009, doi: 10.1016/j.matchemphys.2008.11.005.
- [14] S. Nasresfahani, M. H. Sheikhi, M. Tohidi, and A. Zarifkar, "Methane gas sensing properties of Pd-doped SnO₂/reduced graphene oxide synthesized by a facile hydrothermal route," *Mater. Res. Bull.*, vol. 89, pp. 161–169, May 2017, doi: 10.1016/j.materresbull.2017.01.032.
- [15] J. Kroutil *et al.*, "Performance Evaluation of Low-Cost Flexible Gas Sensor Array with Nanocomposite Polyaniline Films," *IEEE Sens. J.*, vol. 18, no. 9, pp. 3759–3766, May 2018, doi: 10.1109/JSEN.2018.2811461.
- [16] J. Wang, H. qing Fan, H. wa Yu, and X. Wang, "Synthesis and Optical Properties of SnO₂ Structures with Different Morphologies via Hydrothermal Method," *J. Mater. Eng. Perform.*, vol. 24, no. 9, pp. 3426–3432, Sep. 2015, doi: 10.1007/s11665-015-1637-4.
- [17] P. Manjula, L. Satyanarayana, Y. Swarnalatha, and S. V. Manorama, "Raman and MASNMR studies to support the mechanism of low temperature hydrogen sensing by Pd doped mesoporous SnO₂," *Sensors Actuators, B Chem.*, vol. 138, no. 1, pp. 28–34, Apr. 2009, doi: 10.1016/j.snb.2009.02.051.
- [18] H. C. Choi, Y. M. Jung, and S. Bin Kim, "Size effects in the Raman spectra of TiO₂ nanoparticles," *Vib. Spectrosc.*, vol. 37, no. 1, pp. 33–38, Jan. 2005, doi: 10.1016/j.vibspec.2004.05.006.
- [19] D. Yoo, J. J. Lee, C. Park, H. H. Choi, and J. H. Kim, "N-type organic thermoelectric materials based on polyaniline doped with the aprotic ionic liquid 1-ethyl-3-methylimidazolium ethyl sulfate," *RSC Adv.*, vol. 6, no. 43, pp. 37130–37135, Apr. 2016, doi: 10.1039/c6ra02334g.
- [20] W. Chen, Q. Zhou, T. Gao, X. Su, and F. Wan, "Pd-doped SnO₂-based sensor detecting characteristic fault hydrocarbon gases in transformer oil," *J. Nanomater.*, vol. 2013, 2013, doi: 10.1155/2013/127345.
- [21] W. Wan, Y. Li, X. Ren, Y. Zhang, F. Gao, and H. Zhao, "2D SnO₂ nanosheets: Synthesis, characterization, structure, and excellent sensing performance to ethylene glycol," *Nanomaterials*, vol. 8, no. 2, Feb. 2018, doi: 10.3390/nano8020112.
- [22] A. Mirzaei *et al.*, "An overview on how Pd on resistive-based nanomaterial gas sensors can enhance response toward hydrogen gas," *International Journal of Hydrogen Energy*, vol. 44, no. 36. Elsevier Ltd, pp. 20552–20571, Jul. 26, 2019, doi: 10.1016/j.ijhydene.2019.05.180.
- [23] S. Srivastava, S. Kumar, and Y. K. Vijay, "Preparation and characterization of tantalum/polyaniline composite based chemiresistor type sensor for hydrogen gas sensing application," in *International Journal of Hydrogen Energy*, Feb. 2012, vol. 37, no. 4, pp. 3825–3832, doi: 10.1016/j.ijhydene.2011.04.155.
- [24] N. Bafandeh, M. M. Larijani, and A. Shafiekhani, "Investigation on hydrogen sensing property of MWCNT/Pani nanocomposite films," *Polym. Bull.*, vol. 77, no. 7, pp. 3697–3706, Jul. 2020, doi: 10.1007/s00289-019-02915-8.
- [25] L. Al-Mashat *et al.*, "Graphene/polyaniline nanocomposite for hydrogen sensing," *J. Phys. Chem. C*, vol. 114, no. 39, pp. 16168–16173, Oct. 2010, doi: 10.1021/jp103134u.

- [26] A. Z. Sadek *et al.*, “A room temperature polyaniline nanofiber hydrogen gas sensor,” *Proc. IEEE Sensors*, vol. 2005, pp. 207–210, 2005, doi: 10.1109/ICSENS.2005.1597672.
- [27] N. D. Sonwane, M. D. Maity, and S. B. Kondawar, “Conducting polyaniline/SnO₂ nanocomposite for room temperature hydrogen gas sensing,” in *Materials Today: Proceedings*, Jan. 2019, vol. 15, pp. 447–453, doi: 10.1016/j.matpr.2019.04.106.
- [28] H. J. Sharma, D. V. Jamkar, and S. B. Kondawar, “Electrospun Nanofibers of Conducting Polyaniline/Al-SnO₂ Composites for Hydrogen Sensing Applications,” *Procedia Mater. Sci.*, vol. 10, pp. 186–194, Jan. 2015, doi: 10.1016/j.mspro.2015.06.040.
- [29] S. Srivastava, S. Kumar, V. N. Singh, M. Singh, and Y. K. Vijay, “Synthesis and characterization of TiO₂ doped polyaniline composites for hydrogen gas sensing,” *Int. J. Hydrogen Energy*, vol. 36, no. 10, pp. 6343–6355, May 2011, doi: 10.1016/j.ijhydene.2011.01.141.
- [30] I. H. Kadhim and H. A. Hassan, “Room temperature hydrogen gas sensor based on nanocrystalline SnO₂ thin film using sol–gel spin coating technique,” *J. Mater. Sci. Mater. Electron.*, vol. 27, no. 5, pp. 4356–4362, May 2016, doi: 10.1007/s10854-016-4304-0.
- [31] J. M. Lee *et al.*, “Ultra-sensitive hydrogen gas sensors based on Pd-decorated tin dioxide nanostructures: Room temperature operating sensors,” *Int. J. Hydrogen Energy*, vol. 35, no. 22, pp. 12568–12573, Nov. 2010, doi: 10.1016/j.ijhydene.2010.08.026.

Graphical Abstract

Highlights for the Review

- In this work, we report a unique hybrid composite film fabricated with the novel nanocomposite film based on tin oxide (SnO₂) nanosheets with polyaniline (PANI) doped with palladium (Pd) for room temperature hydrogen sensor.
- Using first-principles density functional theory, the effects of gas adsorption on the electronic and transport properties of the sensor are examined. The computations show that the sensitivity of the SnO₂ to the H₂ gas molecules is considerably improved after hybridisation with Pd and, the sensitivity of the PANI to the H₂ gas molecules is considerably improved after hybridisation with SnO₂.
- The highest sensitivity among all the films at room temperature has been observed as ~540% for the SnO₂/Pd film at 0.4% of the target gas and performance factor (the ratio of response percentage to total cycle time) is evaluated highest in Pd doped PANI-SnO₂ film.
- Our results reveal the promising future of SnO₂, PANI and Pd associated hybrid films in the development of ultra-high sensitive gas sensors.